Hyaluronidase-4 is produced by mast cells and can cleave serglycin chondroitin sulfate chains into lower molecular weight forms

Received for publication, March 28, 2019, and in revised form, May 29, 2019 Published, Papers in Press, June 7, 2019, DOI 10.1074/jbc.RA119.008647

Brooke L. Farrugia[‡§1], Shuji Mizumoto[¶], Megan S. Lord[§], Robert L. O'Grady[§], Rhiannon P. Kuchel[‖], Shuhei Yamada[¶], and John M. Whitelock[§]

From the [‡]Department of Biomedical Engineering, The University of Melbourne, Victoria 3010, Australia, [§]Graduate School of Biomedical Engineering, UNSW, Sydney, NSW 2052 Australia, [¶]Department of Pathobiochemistry, Faculty of Pharmacy, Meijo University, 150 Yagotoyama, Tempaku-ku, Nagoya 468-8503, Japan, and [‖]Electron Microscope Unit, UNSW, Sydney, NSW 2052 Australia

Edited by Gerald W. Hart

Mast cells represent a heterogeneous cell population that is well-known for the production of heparin and the release of histamine upon activation. Serglycin is a proteoglycan that within mast cell α-granules is predominantly decorated with the glycosaminoglycans heparin or chondroitin sulfate (CS) and has a known role in granule homeostasis. Heparanase is a heparin-degrading enzyme, is present within the α-granules, and contributes to granule homeostasis, but an equivalent CS-degrading enzyme has not been reported previously. In this study, using several approaches, including epitope-specific antibodies, immunohistochemistry, and EM analyses, we demonstrate that human HMC-1 mast cells produce the CS-degrading enzymes hyaluronidase-1 (HYAL1) and HYAL4. We observed that treating the two model CS proteoglycans aggrecan and serglycin with HYAL1 and HYAL4 *in vitro* cleaves the CS chains into lower molecular weight forms with nonreducing end oligosaccharide structures similar to CS stub neoepitopes generated after digestion with the bacterial lyase chondroitinase ABC. We found that these structures are associated with both the CS linkage region and with structures more distal toward the nonreducing end of the CS chain. Furthermore, we noted that HYAL4 cleaves CS chains into lower molecular weight forms that range in length from tetra- to dodecasaccharides. These results provide first evidence that mast cells produce HYAL4 and that this enzyme may play a specific role in maintaining α-granule homeostasis in these cells by cleaving CS glycosaminoglycan chains attached to serglycin.

Mast cells are a heterogeneous population of cells, well-known for the release of histamine on activation, as well as the production of heparin (1). Histamine, along with a myriad of molecules from growth factors, chemokines, and proteases, are stored in the α-granules of mast cells (2). These molecules are protected within the α-granules by the glycosaminoglycan (GAG)[2] chains that decorate the proteoglycan (PG) serglycin (2). The storage of histamine and serotonin in mast cell granules depends on the presence of serglycin (3), specifically its GAG chains (4–6). The GAG chains that decorate mast cell serglycin vary depending on the species and origin of the tissue (7). Mast cell serglycin may be decorated with heparin (1, 8), a mixture of oversulfated chondroitin sulfate (CS), and heparin/heparan sulfate (HS) (9, 10) or exclusively with CS (11, 12). On activation, mast cells release the contents of their α-granules into the surrounding tissue, also known as degranulation. The difference in pH between the α-granule and the surrounding tissue is one mechanism that facilitates the release of mediators from the GAG chains within the granules to the surrounding tissue because of the change in electrostatic interaction (13). The depolymerization of GAG chains also aids in the release of proteases into the surrounding tissue on α-granule degranulation, with partial depolymerization of HS/heparin by heparanase facilitating release of proteases (14), although an equivalent enzyme for the depolymerization of CS produced by mast cells has yet to be reported.

CS consists of the repeating disaccharide structure of -4GlcUAβ1−3GalNAcβ1- (GlcUA = D-glucuronic acid and GalNAc = *N*-acetyl-D-galactosamine). The repeating disaccharide structure may be sulfated at one or multiple positions, with *O*-sulfation at C2 on GlcUA and four and/or six positions on GalNAc. CS disaccharide structures are commonly referred to as CS-A (GlcUA-GalNAc(4S)), CS-B (GlcUA(2S)-GalNAc(4S)), CS-C (GlcUA-GalNAc(6S)), CS-D (GlcUA(2S)-GalNAc(6S)), CS-E (GlcUA-GalNAc(4S,6S)), and CS-T (GlcUA(2S)-GalNAc(4S,6S)), where 2S, 4S, and 6S represent 2-*O*-sulfate, 4-*O*-sulfate, and 6-*O*-sulfate, respectively. The study of these structures is aided by several monoclonal antibodies against specific CS chain disaccharides. The antibody clone CS-56 recognizes CS-A and CS-D disaccharide motifs (15, 16). CS-D can also be recognized by the antibody clone MO-225 (17). CS-E has also been shown to be recognized by the mAb clones E-12C and E-18H (18). In addition to CS disaccharide chain structures, several monoclonal antibodies, referred to as anti-CS

The authors declare that they have no conflicts of interest with the contents of this article.

[1] To whom correspondence should be addressed. Tel.: 61-3-8344-6165; E-mail: brooke.farrugia@unimelb.edu.au.

[2] The abbreviations used are: GAG, glycosaminoglycan; C'ase, chondroitinase; CS, chondroitin sulfate; ddH_2O, double distilled H_2O; Gal, D-galactose; HA, hyaluronan; PG, proteoglycan; PMA, phorbol 12-myristate 13-acetate; SG buffer, Siriganian activation buffer: 119 mM NaCl, 5 mM KCl, 25 mM PIPES, 5.6 mM dextrose, 0.4 mM $MgCl_2$, pH 7.25; TBST, Tris-buffered saline with Tween 20; Xyl, D-xylose; HS, heparan sulfate.

stub antibodies, were developed against bacteria-derived chondroitinase (C'ase) ABC generated "neo"-stub epitope structures (19, 20). Exhaustive treatment of a CS-decorated PG with bacterial C'ase ABC generates terminal unsaturated disaccharide structures, ΔHexUA-GalNAc, following the linkage region tetrasaccharide (GlcUA-Gal-Gal-Xyl) (Gal = D-galactose, Xyl = D-Xylose). The anti-CS neo-stub antibodies 1B5, 2B6, 3B3 detect the terminal unsaturated ΔHexUA-GalNAc(0S), ΔHexUA-GalNAc(4S), or ΔHexUA-GalNAc(6S), respectively. The antibody clone 3B3 also detects a nonreducing, terminal saturated CS disaccharide, GlcUA-GalNAc(6S) not generated by C'ase ABC treatment (21), commonly referred to as 3B3(−). Similarly, clone 2B6 detects a CS chain structure in the absence of C'ase ABC in rodent-derived mast cells, referred to as 2B6(−) (22); however, the epitope has not been reported.

Although the biosynthesis of CS is well-known, the mammalian enzymes responsible for its turnover in tissues are not well-defined. Cellular degradation of CS occurs in the lysosomes and is a highly ordered process that depends on specific hydrolases (23). Degradation of CS starts with the catabolism of the polysaccharide chain by endolytic cleavage. The polysaccharide chain is then degraded into smaller saccharide units via multiple sulfatases and exoglycosidases (23). The family of hyaluronidases (HYAL), of which there are six members, HYAL1, HYAL2, HYAL3, HYAL4, SPAM1 (PH-20), and HYALP1, were named because of their ability to degrade hyaluronan (HA) (23), although a number of them have also been shown to degrade CS (24). Human HYAL1 and testicular hyaluronidase (SPAM1) degrade CS as well as HA to a similar extent (25), whereas HYAL4 has specificity toward CS-C and CS-D (24), but not HA. HYAL1 is ubiquitously expressed, whereas HYAL4 has only been shown to be synthesized in placentae, skeletal muscle (26), and testis (24). Both HYAL and C'ase ABC cleave CS at the GalNAcβ1→4GlcUA linkage; however, HYAL is a hydrolase, generating a terminal saturated disaccharide structure, whereas C'ase ABC is an eliminase that generates a terminal unsaturated structure.

This study demonstrated the production of the CS depolymerizing enzymes HYAL1 and HYAL4 by mast cells and is the first report of a mammalian CS depolymerization enzyme produced by mast cells. Specially, this study demonstrated that HYAL4 can degrade the CS attached to the proteoglycans serglycin and aggrecan.

Results

CS produced by mast cells

The CS produced by mast cells was explored using the HMC-1 cell line by flow cytometry (Fig. 1, *A* and *B*). HMC-1 cells expressed CS with epitopes detected by the antibody clone CS-56 (Fig. 1*A*). The level of this epitope varied depending on the activation state and whether the cells were permeabilized, demonstrating a difference in expression of CS chains after activation, and whether the epitope was cell surface–associated or intracellular. HMC-1 cells also expressed CS with the 2B6(−) epitope (Fig. 1*B*). The level of this epitope varied slightly depending on the activation state of the mast cells, with a slight increase compared with the experimental controls (cells alone or probed with mouse Ig). The localization of the 2B6(−) epitope in mast cells was further explored using immuno-EM (Fig. 1*C*). Immunolocalization of the 2B6(−) epitope was ubiquitous throughout the mast cell being associated with multiple cell organelles (Fig. 1*C*, *i*, *black arrows*), the cell cytoplasm (Fig. 1*C*, *i*, *white arrows*), and multiple regions within the cell nucleus (Fig. 1*C*, *ii*, *dark region*, *black arrows*; *light region*, *white arrows*). No immunoreactivity was detected within the negative controls using gold nanoparticle-conjugated secondary antibodies in the absence of the primary antibody, supporting the specificity of the 2B6(−) reactivity.

Mast cells were identified in the dermis of human skin via toluidine blue staining (Fig. 2*A*) and immunolocalization of mast cell tryptase (Fig. 2*B*). CS was also detected in the dermis as detected by the anti-CS antibody clone 2B6 following C'ase ABC digestion that detected 4-sulfated CS stubs and this antibody without C'ase ABC treatment (2B6(−)) (Fig. 2, *C* and *D*). The 4-sulfated CS stub (2B6(+)) was localized throughout the dermis, with cells stained more intensely than the surrounding tissue (Fig. 2*C*, indicated by *black arrows*). In contrast, the 2B6(−) epitope was detected in cells of similar localization and morphology (Fig. 2*D*, indicated by *black arrows*) as mast cells (Fig. 2, *A* and *B*). CS detected by antibody clone 3B3 either with or without C'ase ABC treatment was not present in the skin tissue (Fig. 2, *E* and *F*) whereas no reactivity was observed for the isotype control (Fig. 2*G*). These results suggested that mast cells possessed CS with a unique CS chain structure that may be the result of processing of the CS chain.

Mast cells produce HYAL1 and HYAL4

To explore whether mast cells produced enzymes capable of cleaving CS chains, the expression of HYAL1 and HYAL4 by HMC-1 cells was explored. HMC-1 cells were found to express both HYAL4 (Fig. 3, *A* and *B*) and HYAL1 (Fig. 3, *C* and *F*) as determined by flow cytometry. The expression of HYAL4 by nonpermeabilized cells (Fig. 3*A*) was greater than for permeabilized cells as indicated by a shift in the fluorescence level (Fig. 3*B*), suggesting HYAL4 was associated with the cell surface. In contrast, HYAL1 was detected in the permeabilized cells (Fig. 3*D*) but not the nonpermeabilized cells (Fig. 3*C*). In addition, HMC-1 cell lysate was analyzed for the presence of HYAL4 by Western blotting (Fig. 3*E*). A band at ~55,000 relative molecular mass (M_r) was detected, indicating the presence of HYAL4. Human dermal tissue was also probed for the presence of HYAL4, which was detected within the dermis and the basal region of the epithelium (Fig. 3*F*). These data demonstrate that mast cells produce the CS depolymerizing enzymes HYAL1 and HYAL4 that may be responsible for generating the 2B6(−) reactivity demonstrated in HMC-1 cells and human dermal tissue.

HYAL1 and HYAL4 depolymerize CS chains that decorate CSPGs

Having established that mast cells produce HYAL1 and HYAL4, it was of interest to determine whether depolymerization of CS by these enzymes would result in the generation of unique CS epitopes, such as those detected with the CS stub antibodies 2B6 and 3B3. Model CSPGs, ACAN and SGN were

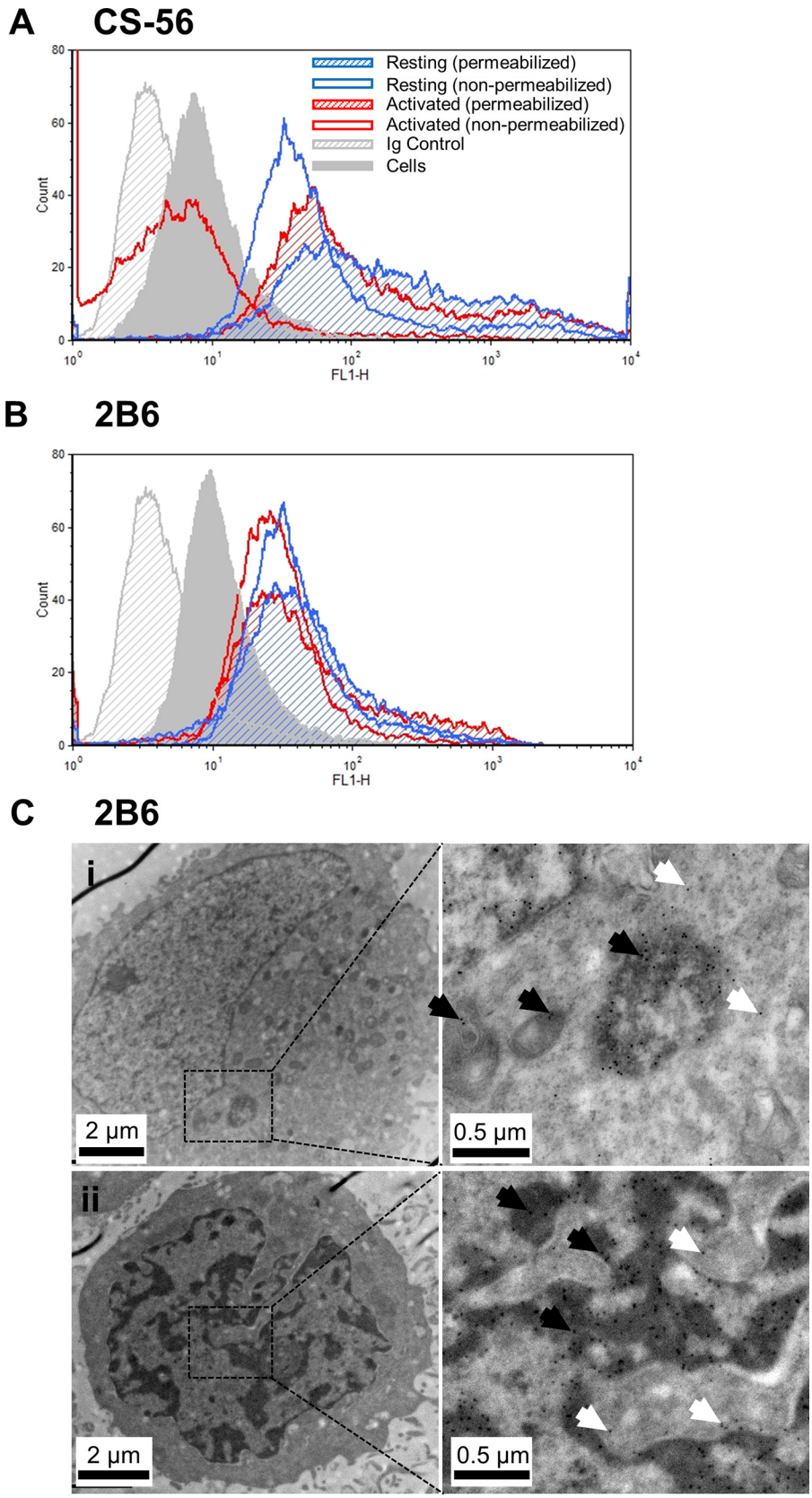

Figure 1. CS expression and localization by mast cells. *A* and *B*, expression of CS (clone CS-56) (*A*) and 2B6 (−) (*B*) by HMC-1 cells as determined by flow cytometry for nonpermeabilized and permeabilized cells compared with cell alone or isotype control. *C*, immunolocalization of CS using clone 2B6(−) in HMC-1 cells determined by immune-TEM ubiquitously throughout the cell, including multiple cell organelles (*i insert*, indicated by *black arrows*), and cytoplasm (*i insert*, indicated by *white arrows*) and multiple regions within the cell nucleus including the dark region (*ii insert*, indicated by *black arrows*), and light region (*ii insert*, indicated by *white arrows*).

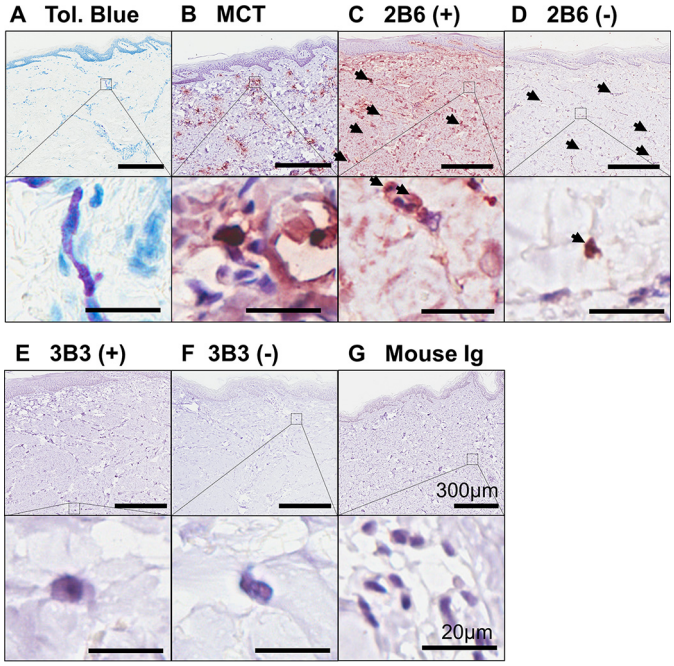

Figure 2. Localization of mast cells and CS in human dermal tissue. *A–G*, sections were characterized by staining with toluidine blue that indicates mast cells in *magenta* (*A*), mast cell tryptase (*B*), CS detected by 2B6(+) (*C*), 2B6(−) (*D*), 3B3(+) (*E*), 3B3(−) (*F*), and mouse IgG (*G*). Positive (+) and negative (−) indicate tissue sections with and without treatment with C'ase ABC prior to antibody probing. *Arrows* indicate cells of interest. *Scale bar* in low magnification images = 300 μm and high magnification images = 20 μm.

treated with recombinant human HYAL1 and mouse HYAL4 (Fig. 4, *A*, *C*, and *E*), and recombinant human HYAL4 (Fig. 4, *B*, *D*, and *F*). Confirmation of CS depolymerization was demonstrated by ELISA following HYAL treatment of CSPGs ACAN and SGN, as measured by the loss of immunoreactivity of CS-56 epitopes, suggesting loss of CS chains that decorate ACAN (Fig. 4*A*) and SGN (Fig. 4*B*). Experimental controls, in the absence of enzyme treatment, showed presence of CS chain epitopes in both ACAN and SGN samples. Following the treatment with C'ase ABC, the presence of CS chain epitopes were decreased in both ACAN and SGN samples. Similarly, when ACAN and SGN were subject to either HYAL1 or HYAL4 treatment, immunoreactivity of CS chain epitopes was decreased as compared with the nondigested samples.

To investigate the generation of CS epitopes detected by the monoclonal antibodies 2B6 and 3B3, ACAN (Fig. 4, *C* and *E*) and SGN (Fig. 4, *D* and *F*) were treated with C'ase ABC, HYAL1, or HYAL4 and probed for the presence of 2B6 (Fig. 4, *C* and *D*) or 3B3 (Fig. 4, *E* and *F*) epitope structures using ELISA. Treatment of ACAN with C'ase ABC generated epitopes that were detected with the antibody clone 2B6, whereas treatment with either HYAL1 or HYAL4 did not (Fig. 4*C*). Similar to ACAN, treatment of SGN with C'ase ABC generated epitopes detected with the antibody clone 2B6, whereas HYAL4 did not (Fig. 4*D*). Treatment of ACAN with either C'ase ABC, HYAL1, or HYAL4 generated epitope structures that were detected with the antibody clone 3B3 (Fig. 4*E*). Following treatment of SGN with C'ase ABC or HYAL4, epitopes detected by the antibody clone 3B3 were generated following treatment with HYAL4, whereas they were not generated following treatment with C'ase ABC (Fig. 4*F*). Native epitopes detected by antibody clones 2B6 or 3B3 on CS that decorated SGN were not evident, as demonstrated by no reactivity when probing for the antibody epitopes in the absence of enzyme treatment (control) (Fig. 4, *D* and *F*). Immunoreactivity toward the 1B5 epitope was not detected following treatment of ACAN or SGN with C'ase ABC, HYAL1, or HYAL4 (data not shown) and was not examined further in this study. These data demonstrate that following depolymerization of CS chains that decorate CSPGs by both C'ase ABC and HYAL, structures are generated that can be detected with the CS stub antibodies, suggesting that HYAL may be the enzyme responsible for generating the so-called native CS structures present in mast cells.

To further investigate the depolymerization of CS chains that decorate CSPGs, the presence and generation of CS structures following treatment in time course experiments was evaluated. Results demonstrated both HYAL1 and HYAL4 were produced by mast cells and depolymerized CS, HYAL4 was chosen to further investigate depolymerization of CS chains. Model CSPGs, ACAN and SGN, were treated with C'ase ABC and HYAL4 for up to 720 min at which exhaustive treatment was reached. Following treatment, samples were coated onto high-binding well plates, and depolymerization of CS chains was evaluated by presence of CS-56 epitopes, and generation of CS structures by the presence of 2B6 and 3B3 epitopes (Fig. 5). Following treatment of ACAN with C'ase ABC, immunoreactivity of CS-56 epitopes was shown to be constant up to ~300 min, with a decrease in reactivity at 720 min (Fig. 5*A*). Over the period of C'ase ABC treatment of ACAN, the immunoreactivity of the 2B6 and 3B3 epitopes increased (Fig. 5*B*), with the appearance of the 3B3 reactivity being slightly delayed (Fig. 5*C*). Treatment of ACAN with HYAL4 showed CS-56 epitopes decreased over the duration of treatment (Fig. 5*D*), indicating depolymerization of CS chains. This did not correspond with the generation of 2B6 epitopes (Fig. 5*E*); however, the decrease in CS-56 epitopes correlated to an increase in the detection of 3B3 epitopes (Fig. 5*F*). Treatment of SGN with C'ase ABC gave a similar picture to that seen with ACAN, showing a decrease in the immunoreactivity of epitopes detected with antibody CS-56 (Fig. 5*G*), suggesting depolymerization of CS that decorates the SGN protein core. Depolymerization of CS decorating SGN corresponded with the generation of epitopes detected with the antibody clone 2B6 (Fig. 5*H*), whereas the detection of 3B3 epitopes increased at ~240 min (Fig. 5*I*). HYAL4 treatment of SGN resulted in a decrease in CS-56 immunoreactivity from 0 to 60 min, whereas from 60 min onwards the immunoreactivity plateaued, demonstrating depolymerization of CS chains that decorated SGN (Fig. 5*J*). Epitopes detected with the 2B6 antibody were not generated following treatment of SGN with HYAL4 (Fig. 5*K*), however 3B3 epitopes were shown to be generated and immunoreactivity increased up to 120 min, which corresponded with the decrease of CS-56 epitope (Fig. 5*L*). These data further demonstrate depolymerization of CS chains that decorated CPSGs by HYAL4. Surprisingly, these data also demonstrate that structures can be more distal to the linkage region toward the nonreducing end.

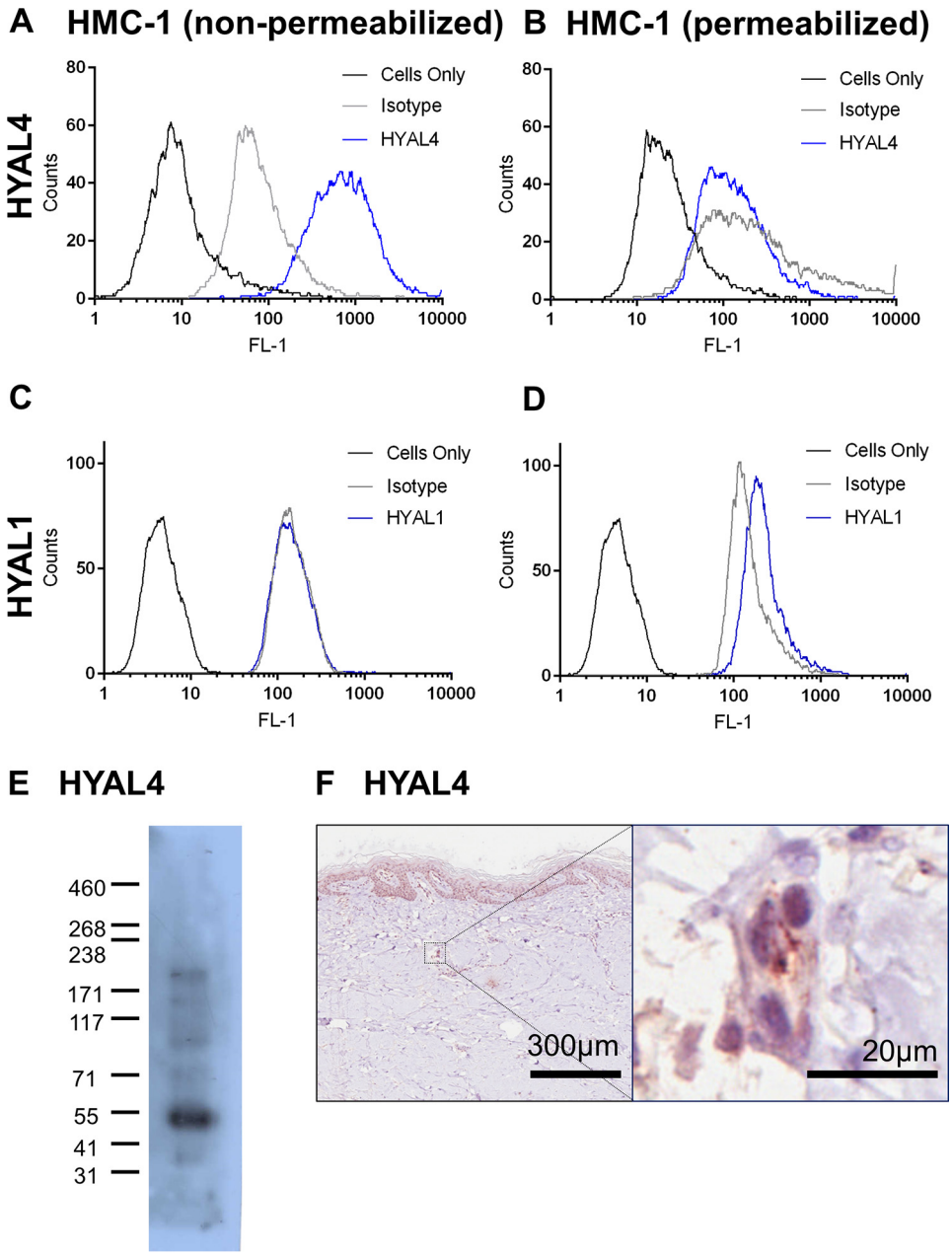

Figure 3. Mast cells produce CS degrading enzymes. *A* and *B*, HYAL4 detected in mast cells by flow cytometry. *A*, cells were not permeabilized prior to probing with HYAL4. *B*, cells were permeabilized prior to probing with HYAL4. *C* and *D*, HMC-1 cells probed for the presence of HYAL1 by flow cytometry. *C*, cells were not permeabilized prior to probing with HYAL4. *D*, cells were not permeabilized prior to probing with HYAL4. *E*, Western blot analysis of HMC1 lysate probed for the presence of HYAL4. *F*, immunolocalization of HYAL4 in human skin.

HYAL1 and HYAL4 depolymerize isolated CS chains

The results presented above suggest that CS structures generated by either C'ase ABC or HYAL and detected by CS antibodies 2B6 or 3B3 can be terminal chain nonreducing structures and are therefore not only associated with the PG linkage region. This was further explored by the treatment of CS chains, in the absence of a protein core, with C'ase ABC or HYALs and the generation of epitopes detected by 2B6 and 3B3 antibody clones. Biotinylated CS, CS-A, and CS-C, attached to streptavidin ELISA plates were treated with HYALs and the immunoreactivity of CS epitopes CS-56, 2B6, and 3B3 was investigated. Detection of CS-56 epitopes on CS-A and CS-C chains decreased following treatment with both HYAL1 and HYAL4, as compared with nontreated CS (Fig. 6*A*). Treatment with HYAL1 increased detection of 2B6 epitopes on CS-A (Fig. 6*B*) and 3B3 epitopes on CS-C (Fig. 6*C*) as compared with CS chains in the absence of HYAL1 treatment. Similar results were shown following treatment with HYAL4, with increased detection of 2B6 epitopes on CS-A (Fig. 6*D*) and 3B3 epitopes on CS-C (Fig. 6*E*), compared with the absence of HYAL treatment. Generation of 2B6 (Fig. 6*F*) and 3B3 epitopes (Fig. 6*G*) on CS-A and CS-C was investigated following treatment with C'ase ABC. Results showed increased detection of 2B6 epitopes on CS-A, and 3B3 on both CS-A and CS-C as compared with samples in the absence of C'ase ABC digestion, further demonstrating the ability of HYAL4 to generate these mAb epitopes in the absence

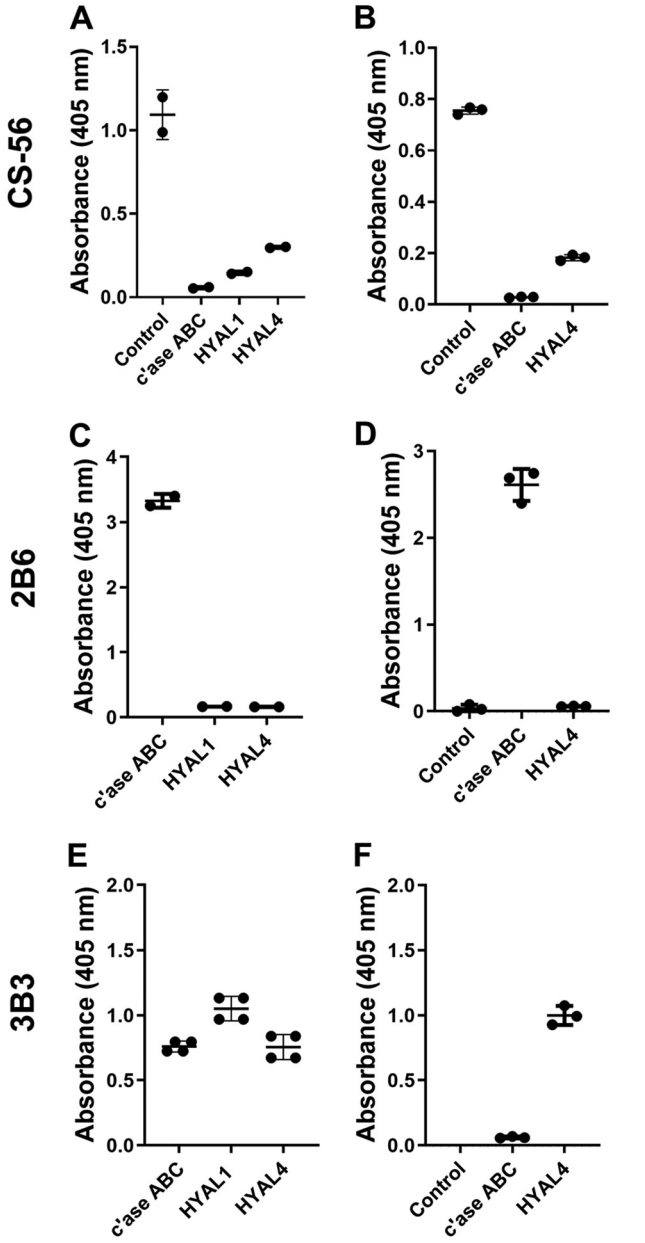

Figure 4. HYAL cleaves CS chains on CSPGs and generates CS cleavage epitopes. *A–F*, expression of CS chain epitopes (CS-56) on aggrecan (ACAN) (*A*) and recombinant serglycin (SGN) (*B*) following C'ase ABC or HYAL digestion, including recombinant human HYAL1 and mouse HYAL4 (*A*, *C*, and *E*) and recombinant human HYAL4 (*B*, *D*, and *F*). Generation of CS stub neoepitopes following C'ase ABC or HYAL digestion of ACAN (*A* and *C*), or SGN (*D* and *F*) detected using the epitopes 2B6 (*C* and *D*) and/or 3B3 (*E* and *F*). Data presented as mean ± S.D.

of the PG linkage region. These data together with the results presented in Fig. 5 demonstrate the exolytic cleavage of CS chains with C'ase ABC generating both 2B6 and 3B3 epitopes over time (Fig. 7*A*), which depends on the CS disaccharide composition of the GAG being analyzed. Thus, the structure present at the nonreducing end may be either ΔHexUA-GlNAc(4S) or ΔHexUA-GlNAc(6S). However, absence of the 2B6 epitope being generated following HYAL4 treatment suggests endolytic cleavage, with preferential cleavage of the β1⟶4 glycosidic bonds with the GlcUA-GlNAc(6S) disaccharide structures on the reducing side (Fig. 7*B*).

HYAL generates lower molecular weight forms of CS

To further evaluate depolymerization of CS by HYAL4 and the CS structures generated following treatment, analysis of diethylaminoethyl-enriched recombinant SGN CS chains (Fig. 8, *A–C*), as well as oligosaccharides from the linkage region (Fig. 8, *D–F*), was carried out. Recombinant SGN was treated with HYAL4 or C'ase ABC, followed by labeling with the fluorophore 2AB and gel filtration on a Superdex peptide column, to obtain CS structures within the CS-disaccharide repeating region. In the absence of treatment (Fig. 8*A*), a peak with a retention time of ~62 min was observed, indicative of excess labeling agent. Treatment with HYAL4 (Fig. 8*B*) yielded multiple peaks that eluted between ~25–38 min. They correspond to CS oligosaccharides that ranged in size from tetra- to dodecasaccharides. Digestion of SGN with C'ase ABC (Fig. 8*C*) resulted disaccharides shown as a peak with retention time of ~44 min. Analysis of the saccharide structures of the linkage region was also performed by gel filtration (Fig. 8, *D–F*) and anion exchange HPLC (Fig. 8, *G–I*). GAG chains were released from the protein core of SGN by alkaline treatment and the reducing end was labeled with 2AB. The labeled GAGs were treated with either HYAL4 or C'ase ABC and analyzed. Nontreated CS (Fig. 8*D*) resulted in a peak at the initial void volume (~20 min) indicative of nondigested GAG chains. Peaks were also observed at ~40, 42, and 48 min, although these peaks were also observed for the treated samples. Therefore, they were not assigned as a product produced by HYAL4 or C'ase ABC treatment. The size of oligosaccharides from the linkage region of SGN following HYAL4 treatment ranged from hexa- to dodecasaccharides in length (as indicated) (Fig. 8*E*), whereas, the size of oligosaccharides following C'ase ABC treatment were observed to be hexasaccharides (Fig. 8*F*), corresponding to ΔHexUA-GalNAc-GlcUA-Gal-Gal-Xyl-2AB. These data demonstrate that although HYAL4 and C'ase ABC cleave CS at the GalNAcβ1⟶4GlcUA linkage, HYAL4 requires a different structure present for cleavage to occur and is not able to cleave the CS chains as frequently, indicating a more restricted cleavage site specificity.

Oligosaccharides at the linkage region of SGN were further analyzed via anion exchange HPLC (Fig. 8, *G–I*). In the absence of treatment (Fig. 8*G*), peaks were observed at early retention times (~15–25, 32 min); these peaks were also observed following treatment with both HYAL4 and C'ase ABC at similar retention times and peak intensity, suggesting that they had been present during preparation of the sample. Oligosaccharides present at the linkage region of SGN following treatment with HYAL4 (Fig. 8*H*) were observed at the retention times of the linkage region standards ΔHexUA-GalNAc-GlcUA-Gal-Gal-Xyl (*b*), ΔHexUA-GalNAc-GlcUA(6S)-Gal-Gal-Xyl (*c*), ΔHexUA-GalNAc-GlcUA(4S)-Gal-Gal-Xyl (*d*), and ΔHexUA-GalNAc(4S)-GlcUA-Gal-Gal-Xyl(2P) (*e*); however, as HYAL4 is an hydrolase the ΔHexUA would be a GlcUA. Peaks were also observed at ~45 min and ~52 min and were predicted to be disulfated (†) and trisulfated hexasaccharide (‡) structures respectively. A similar profile was observed of oligosaccharides within the linkage region of SGN following C'ase ABC treatment (Fig. 8*I*). As the disaccharide composition of GAG chains

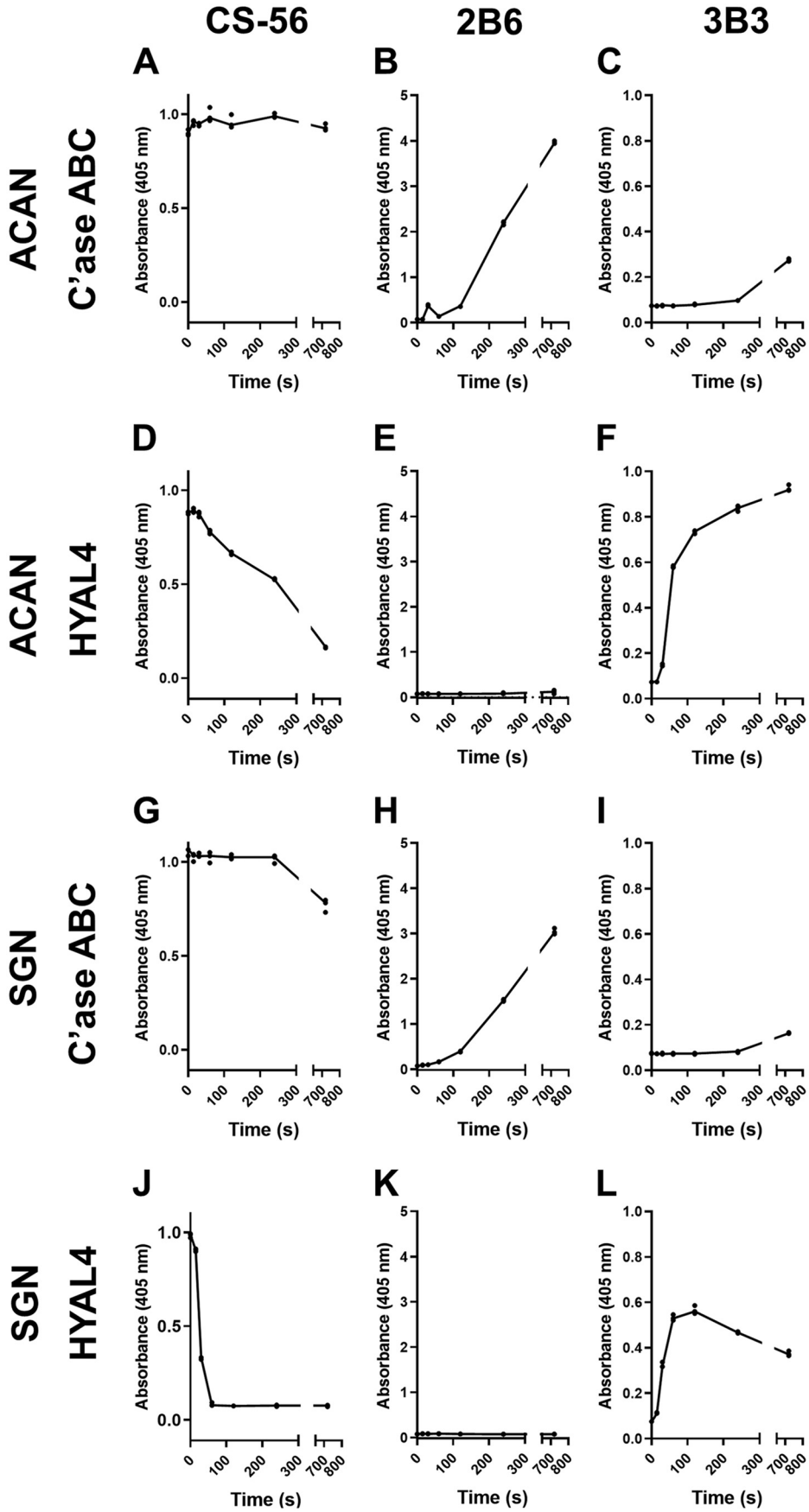
CS-56
2B6
3B3
A
B
C
D
E
F
G
H
I
J
K
L
ACAN
C'ase ABC
ACAN
HYAL4
SGN
C'ase ABC
SGN
HYAL4
Absorbance (405 nm)
Time (s)
0
100
200
300
700
800

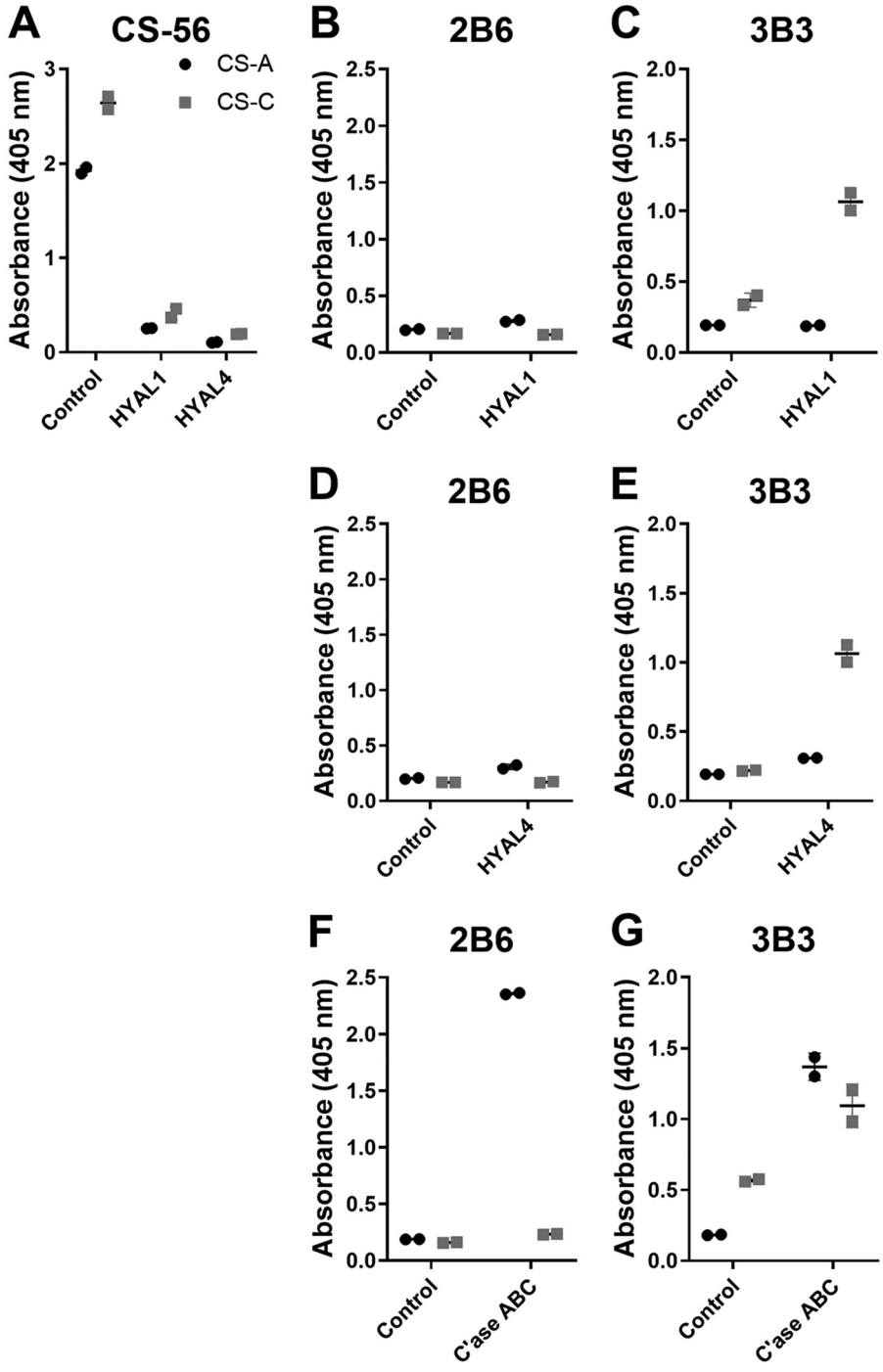

Figure 6. HYAL generates CS cleavage epitopes on CS chains. *A*, presence of CS chain epitopes detected with antibody clone CS-56 following HYAL digestion. *B–G*, biotinylated CS-A and CS-C were treated with HYAL1 (*B* and *C*), HYAL4 (*D* and *E*), or C'ase ABC (*F* and *G*) and probed for the presence of epitopes detected with the antibody clones 2B6 (*B*, *D*, and *F*) or 3B3 (*C*, *E*, and *G*). Control indicates no enzyme treatment. Data presented as mean ± S.D.

is heterogeneous, the oligosaccharide structures at the linkage region were also evaluated after HYAL4 treatment of PG derived from salmon nasal cartilage was also evaluated (Fig. 9). A peak corresponding to the void volume was observed for nontreated samples analyzed by gel filtration HPLC (Fig. 9*A*). Analysis of samples treated with HYAL4 revealed oligosaccharides ranging from hexa- to dodecasaccharides in length (Fig. 9*B*), whereas C'ase ABC treatment generated hexasaccharides (Fig. 9*C*). Oligosaccharides at the linkage region of PG derived from salmon nasal cartilage were further analyzed via anion exchange HPLC (Fig. 9, *D–F*). In the absence of treatment (Fig. 9*D*), no peaks were observed. After HYAL4 treatment (Fig. 9*E*),

Figure 5. Depolymerization of CSPGs, removal of CS chain epitopes and generation of CS cleavage epitopes. *A–L*, depolymerization of CS that decorates the PGs ACAN (*A–F*) and SGN (*G–L*) by C'ase ABC (*A–C* and *G–I*) and HYAL4 (*D–F* and *J–L*) over a period of 12 h demonstrating loss of CS chain epitopes through the detection of CS-56 mAb epitope and generation of CS cleavage epitopes through detection of 2B6 and 3B3 mAb epitopes.

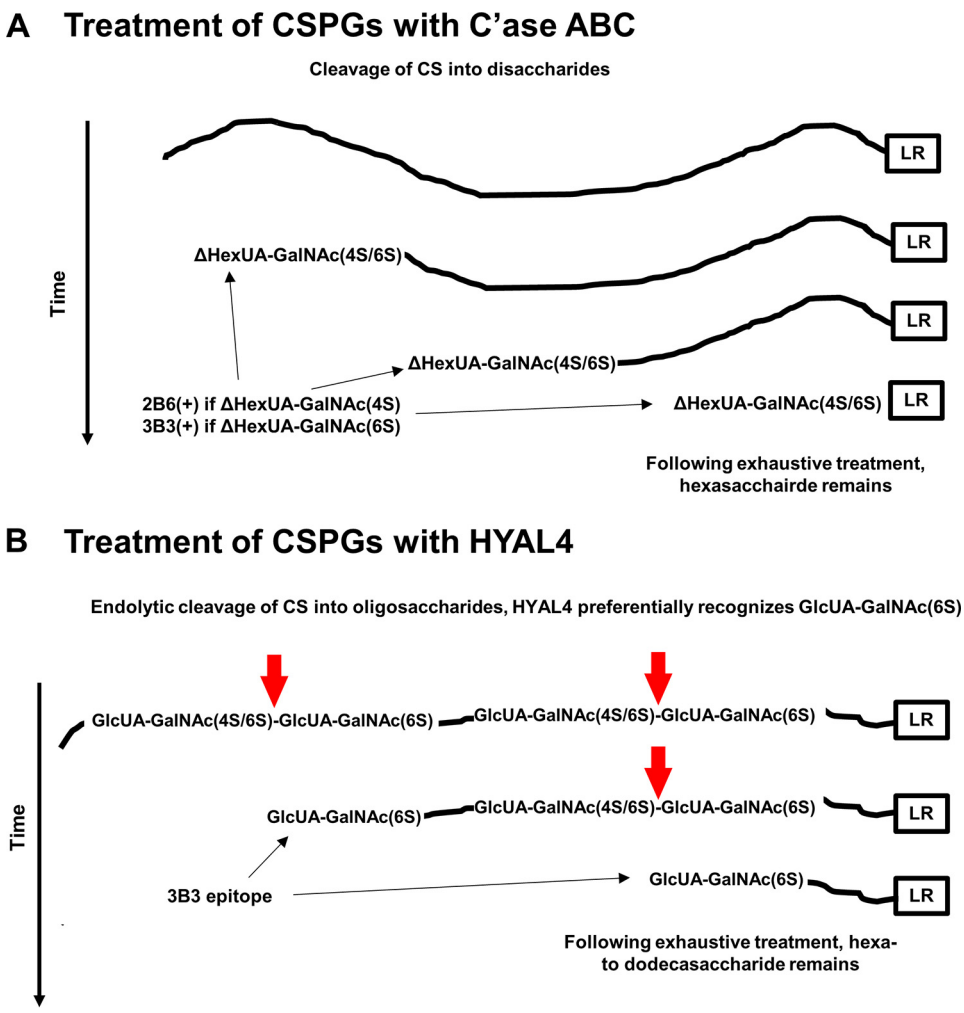

Figure 7. Schematic of CS structures generated by treatment of CSPGs with C'ase ABC or HYAL4. *A*, treatment of a CSPG with C'ase ABC will result in cleavage of the CS chain into disaccharides. Over time the chain will get shorter until exhaustive treatment. Epitopes generated at the nonreduced end will depend on sulfation position on GalNAc immediately following ΔHexUA. *B*, treatment of a CSPG with HYAL4 will result in endolytic cleavage of CS into oligosaccharides, where HYAL4 preferentially cleaves the β1→4 linkage on the nonreducing side of the GlcUA-GalNAc(6S) structure (indicated by the *red arrows*). The size of the oligosaccharides will depend on the presence of this cleavage site. Following exhaustive treatment, the remaining structure may be a hexasaccharide or larger oligosaccharides, depending on the position of the innermost cleavage site along CS toward the linkage region tetrasaccharide (*LR*)

peaks were observed at the elution positions corresponding to the linkage region standards ΔHexUA-GalNAc-GlcUA-Gal-Gal-Xyl (*b*), ΔHexUA-GalNAc-GlcUA(6S)-Gal-Gal-Xyl (*c*), and ΔHexUA-GalNAc-GlcUA(4S)-Gal-Gal-Xyl (*d*). As for the HYAL4-treated SGN, the resulting structures would have GlcUA in place of ΔHexUA at the nonreducing end. Peaks were also observed at ~35, 42, 45, and ~52 min and were predicted to be nonsulfated octasaccharides (¶) and decasaccharides (§), and disulfated (†) and trisulfated hexasaccharides (‡), respectively. Whereas, C'ase ABC treatment (Fig. 9*F*) generated peaks corresponding to ΔHexUA-GalNAc-GlcUA-Gal-Gal-Xyl (*b*), ΔHexUA-GalNAc-GlcUA(6S)-Gal-Gal-Xyl (*c*), and ΔHexUA-GalNAc-GlcUA(4S)-Gal-Gal-Xyl (*d*). These data further confirm the ability of HYAL4 to generate larger CS oligosaccharides probably because of a restricted cleavage site specificity.

Discussion

This study demonstrated the production of CS depolymerizing enzymes from the hyaluronidase (HYAL) family by human-derived mast cells. It was demonstrated that HYAL4 cleaves CS chains into oligosaccharides with low molecular weight. These data suggest that mast cells produce a CS depolymerizing enzyme that may play a part in regulating α-granule mediator storage and degranulation. Additionally, model CSPGs ACAN and SGN were used to investigate CS structures produced by HYAL and demonstrated the generation of structures detected by antibodies (2B6 and 3B3) previously thought to be generated only via treatment of CS by bacterial lyases.

This study demonstrated the depolymerization of CS by C'ase ABC and HYAL4. Both C'ase ABC and HYAL4 cleave the *N*-acetylgalactosaminidic bond at the GalNAcβ1→4GlcUA linkage. C'ase ABC is an eliminase, resulting in a terminal ΔHexUA-GalNAc, whereas HYAL is a hydrolase, generating a terminal GlcUA-GalNAc. Treatment with C'ase ABC results in disaccharides, with no specificity toward the sulfate position around the β1→4 linkage cleavage site, whereas, treatment of CS with generates oligosaccharides including octasaccharides (24). The data presented here demonstrate generation of dodecasaccharides following HYAL4 treatment of SGN and salmon nasal cartilage ACAN. HYAL4 preferentially cleaves

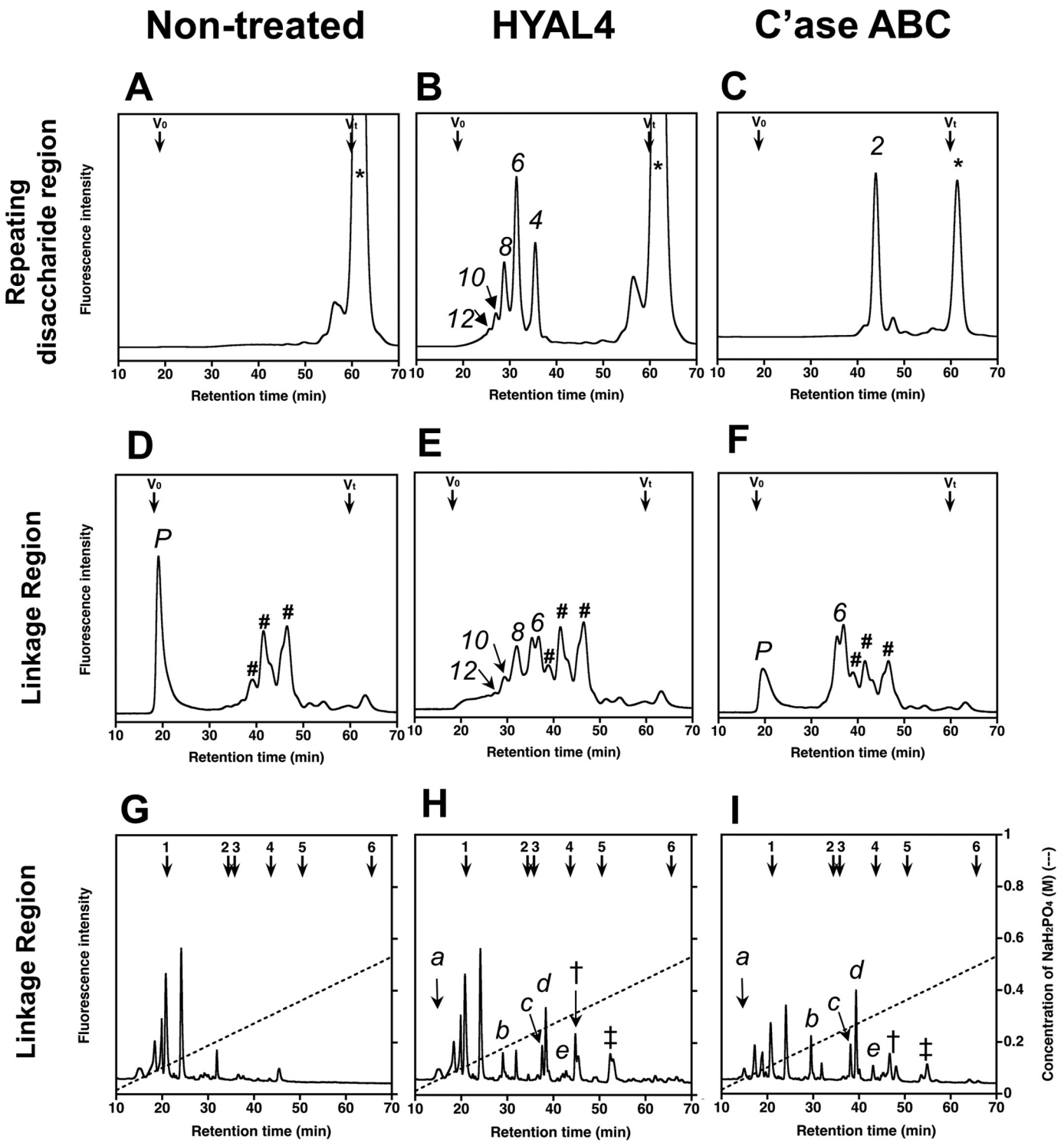

Figure 8. HYAL4 treatment of recombinant serglycin generates oligosaccharides up to dodecasaccharides in length. A–F, gel filtration of 2AB-labeled saccharide structures generated from recombinant SGN. CS chains decorating the SGN protein core were nontreated (*A*) or treated with HYAL4 (*B*) or C'ase ABC (*C*). Saccharide structures were 2AB-labeled and analyzed by gel filtration HPLC on a Superdex peptide column. *D–F*, oligosaccharides from the linkage region of SGN were generated by alkaline treatment, labeled at the reducing end with 2AB (*D*) and treated with HYAL4 (*E*) or C'ase ABC (*F*). *G–I*, oligosaccharides from the linkage region were further analyzed by anion-exchange HPLC following no treatment (*G*), HYAL4 (*H*) or C'ase ABC (*I*) treatment. * indicates excess 2AB labeling reagent, # indicates impurity. Elution positions of 2AB-labeled disaccharide standards are indicated by *numbered arrows* 1 = ΔHexUA-GalNAc, 2 = ΔHexUA-GalNAc(6S), 3 = ΔHexUA-GalNAc(4S), 4 = ΔHexUA(2S)-GalNAc(6S), 5 = ΔHexUA-GalNAc(4S,6S), 6 = ΔHexUA(2S)-GalNAc(4S,6S), and linkage region standards *a* = ΔHexUA-Gal-Gal-Xyl, *b* = ΔHexUA-GalNAc-GlcUA-Gal-Gal-Xyl, *c* = ΔHexUA-GalNAc(6S)-GlcUA-Gal-Gal-Xyl, *d* = ΔHexUA-GalNAc(4S)-GlcUA-Gal-Gal-Xyl, *e* = ΔHexUA-GalNAc-GlcUA-Gal-Gal-Xyl(2P). Based on retention times predicted structures † = disulfated hexasaccharide, ‡ = trisulfated hexasaccharide.

the β1→4 linkage, −GlcUA-GalNAc-GlcUA-GalNAc(6S)− to produce −GlcUA-GalNAc and GlcUA-GalNAc(6S)−, where the 3B3 antibody clone detects GlcUA-GalNAc(6S)−. *In vitro* experiments using ACAN, SGN, CS-A, and CS-D demonstrated the generation of CS structures detected by the antibody clone 3B3, with minimal generation of structures detected by

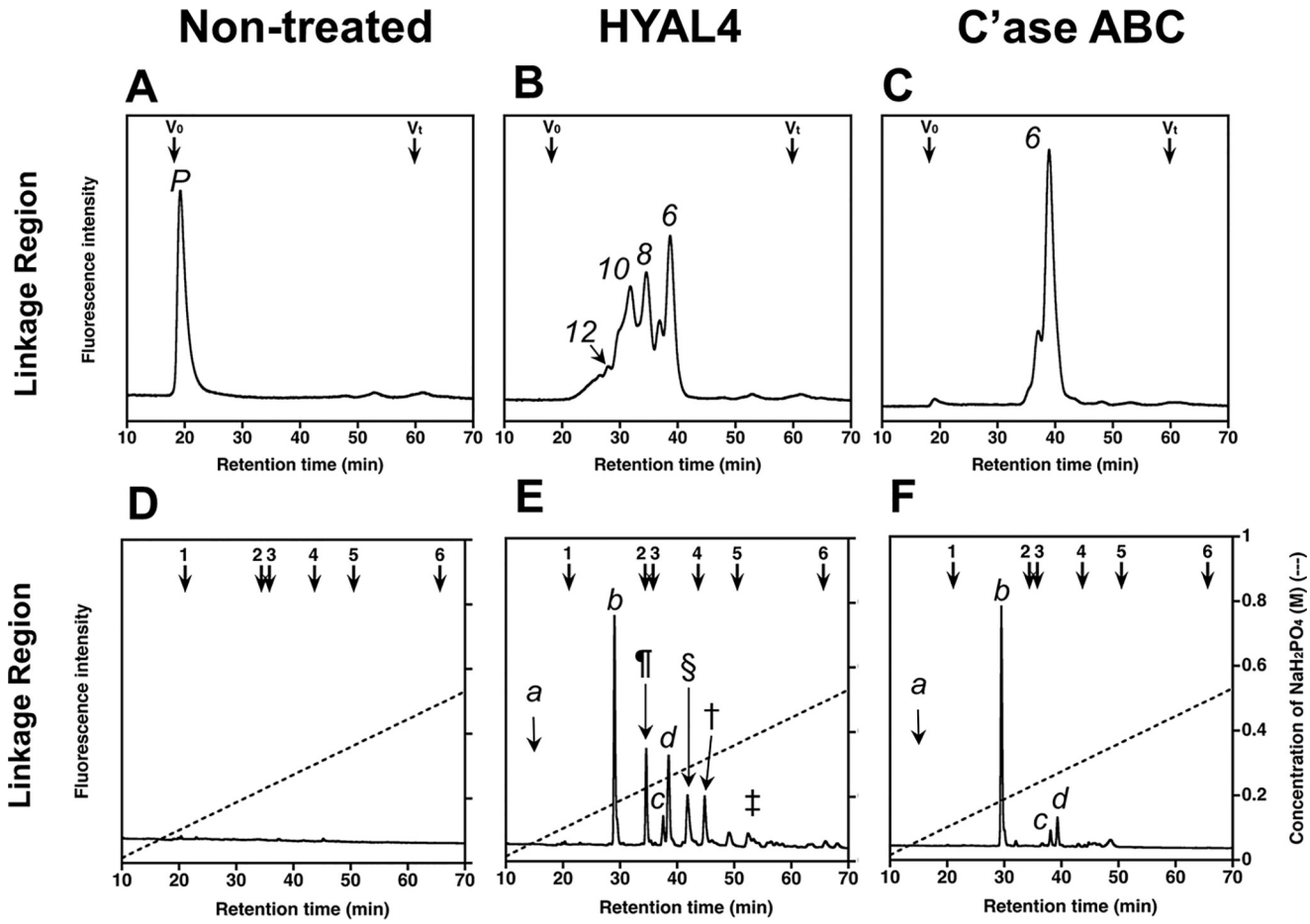

Figure 9. HYAL4 treatment of salmon nasal cartilage generates oligosaccharides up to dodecasaccharides in length. *A–C*, gel filtration of 2AB-labeled saccharide structures generated PG derived from salmon nasal cartilage. Oligosaccharides from the linkage region of the PG were generated by alkaline treatment, labeling the reducing end with 2AB (*A*) and treated with HYAL4 (*B*) or C'ase ABC (*C*). *D–F*, oligosaccharides from the linkage region were further analyzed by anion exchange HPLC following no treatment (*D*) or HYAL4 (*E*) or C'ase ABC (*F*) treatment. Elution positions of 2AB-labeled disaccharide standards are indicated by *numbered arrows* 1 = ΔHexUA-GalNAc, 2 = ΔHexUA-GalNAc(6S), 3 = ΔHexUA-GalNAc(4S), 4 = ΔHexUA(2S)-GalNAc(6S), 5 = ΔHexUA-GalNAc(4S,6S), 6 = ΔHexUA(2S)-GalNAc(4S,6S), and linkage region standards *a* = ΔHexUA-Gal-Gal-Xyl, *b* = ΔHexUA-GalNAc-GlcUA-Gal-Gal-Xyl, *c* = ΔHexUA-GalNAc(6S)-GlcUA-Gal-Gal-Xyl, *d* = ΔHexUA-GalNAc(4S)-GlcUA-Gal-Gal-Xyl, Based on retention times predicted structures † = disulfated hexasaccharide, ‡ = trisulfated hexasaccharide, ¶ = nonsulfated octasaccharide, § = nonsulfated decasaccharide.

the clone 2B6, whereas, analysis of mast cells *in vivo* and *in vitro* (22, 27), as well as the presented data, demonstrated the detection of epitopes recognized by the antibody clone 2B6 in the absence of C'ase ABC, previously referred to as 2B6(−). It was hypothesized that these structures were generated by HYAL4 and may not be native. The native 3B3 epitope, referred to as 3B3(−), identifies progenitor cell populations that play a role in chondrogenesis, intervertebral disc development, and skin morphogenesis (28–30) and is commonly associated with human osteoarthritic cartilage tissue (31). Detection of 2B6(−) has previously been reported in rodent-derived mast cells and tissue (22, 27) and in human osteoarthritic cartilage tissue (32). The presence of mast cells has been demonstrated in both osteoarthritis and rheumatoid arthritis (33), with increased presence in the diseased state as compared with healthy tissue (34). Both 2B6 and 3B3 epitope arthritic tissues may not be a native structure. Rather the presence of these structures, in the absence of C'ase ABC treatment, may indicate the presence of mast cells or the expression of HYAL1 or HYAL4 by other cell types. The *Hyal1* knockout mouse has focused primarily on the effect of HA accumulation (35, 36). The effect on CS structure and accumulation has only been explored in a double knockout with β-hexosaminidase (37). The *Hyal4*-depleted mouse model has yet to be reported in the literature. HA and HYAL are key players in inflammation (38); elevated HYAL has been associated with inflammatory pathologies including rheumatoid arthritis (39), and Hyal1 overexpression linked to immune modulation (40). Given the prevalence of mast cells in inflammatory pathology (41) and the association of the 2B6(−) epitope in osteoarthritis, it will be of interest to observe the effect on mast cell homeostasis and function in not only the *Hyal4*-devoid model but disease-challenged *Hyal*-devoid models.

Partial digestion of ACAN and SGN with C'ase ABC and HYAL4 gave insight into the specificity of HYAL4. Treatment of ACAN and SGN with C'ase ABC generated structures detected with antibody clones 2B6 and 3B3. The concurrent detection of CS chain epitopes suggests the 2B6 and 3B3 epitopes are not required to be adjacent to the linkage region of the CSPG; rather, they can be located distally along the chain toward the nonreducing terminus (Fig. 7). This was further supported by the generation of these structures on CS-A and CS-D

chains in the absence of the PG core protein and linkage region. Treatment of ACAN and SGN with HYAL4 did not result in the generation of 2B6 reactive structures, rather it generated 3B3 reactive structures, suggesting the terminal structure of GlcUA-GalNAc(6S). Because CS that decorates mast cell–derived SGN is predominantly CS-E, the antibody clone 2B6 may react with a terminal disulfated GlcUA-GalNAc(4S,6S) structure in mast cells. The composition of the CS chains that decorate the model CSPGs were highly likely to differ from that of CS that decorates mast cell– derived SGN. As ACAN contains predominantly CS-A (GlcUA-GalNAc(4S)) and CS-C (GlcUA-GalNAc(6S)) disaccharides, and recombinant SGN was reported to be decorated with CS composed of CS-A and CS-D (GlcUA(2S)-GalNAc(6S)) disaccharides (42); therefore, treatment of either ACAN or recombinant SGN with HYAL would generate minimal structures capable of reacting with the antibody clone 2B6.

Mediators within the mast cell α-granules are protected by the GAG chains that decorate SGN, which are predominantly heparin or CS-E, depending on the species and the tissue that the mast cell resides in (13). The interaction between specific GAG chains and mediators has been investigated using a number of different knockout mouse models. SGN-depleted mast cells demonstrated increased disruption to the storage of mediators within the α-granules and absence of tryptase within mast cell extracts (43). Mast cells devoid of heparin because of the depletion of *Ndst2* were not able to store mast cell protease (mMCP)-4, mMCP-5, or carboxypeptidase (5), demonstrating the role this GAG chain plays in the homeostasis of mast cell granule contents. However, depletion of heparin did not eradicate storage of mast cell granule mediators entirely, with expression of mMCP-6 and mMCP-7 observed, suggesting that another GAG in addition to heparin is also responsible for their storage. Depletion of the enzyme, *Galnac4s-6st*, responsible for GalNAc(4S,6S) residues demonstrated reduced expression of mMCP-6 (protein) in mast cells (6), supporting the concept that CS, specifically CS-E, contributes to the storage of mediators within mast cell α-granules. Tryptase is stored within the α-granules as an active tetramer in a complex with GAG chains, with the minimal oligosaccharide length of 8–10 saccharides required for formation of this complex (44). Heparanase, a mammalian endo-β-glucuronidase, is capable of degrading of HS (45) as well as heparin (46). Heparanase within the granules of mast cells has also been shown to maintain granule homeostasis (46) by controlling the degradation of heparin that decorates mast cell SGN. By modifying the size of heparin, heparanase was demonstrated to have an indirect role in regulating the storage of α-granule mediators, as well as in the degranulation process. To date, an equivalent enzyme responsible for the cleavage of mast cell CS has not been reported. Data presented here demonstrated cleavage of CS chains into oligosaccharides. The oligosaccharides ranged from tetra- to dodecasaccharides in length, thus exhibiting the ability to process CS chains into lower molecular weight forms of similar sizes shown to be important in the storage of tryptase as an active tetramer. In summary, we have demonstrated for the first time that mast cells produce the CS-degrading enzymes HYAL1 and HYAL4, supporting the hypothesis that they may be responsible for the cleavage of CS chains that decorated SGN within the mast cell α-granules, and that by cleaving these CS chains may play a role in α-granule homeostasis by regulating mediator storage and degranulation.

Experimental procedures

Materials

C'ase ABC ((EC 4.2.2.4) purified from *Proteus vulgaris* proteinase-free lyase I), C'ase B (EC 4.2.2) purified from *Flavobacterium heparinum*, C'ase ACII purified from *Arthrobacter aurescens*, and heparinase III (EC 4.2.2.8) purified from *F. heparinum* were purchased from Seikagaku Corporation (Tokyo, Japan). Human HYAL1 and mouse HYAL4 were recombinantly produced as described previously (25, 47). Recombinant human HYAL4 was purchased from R&D Systems. Mouse mAbs reactive to the CS stubs following C'ase ABC digestion (clones 1B5, 2B6, and 3B3) were provided by Prof. Bruce Caterson (Cardiff University, Cardiff, UK) and purchased from Comso-Bio (Tokyo, Japan). Anti-mouse and anti-rabbit secondary antibodies were purchased from Merck-Millipore (Sydney, Australia). Secondary HRP-conjugated antibodies were purchased from Dako (Sydney, Australia). All other chemicals were purchased from Sigma-Aldrich, unless otherwise stated.

Culture of HMC-1 cells

HMC-1 cells were maintained in RPMI 1640 medium containing 10% (w/w) FBS and 100 units/ml penicillin and 100 μg/ml of streptomycin and maintained in a humidified incubator (5% CO_2/95% air atmosphere at 37 °C); media were replenished every 3–4 days. Siriganian (SG) activation buffer (119 mM NaCl, 5 mM KCl, 25 mM PIPES, 5.6 mM dextrose, 0.4 mM $MgCl_2$, pH 7.25) was prepared and filter sterilized and 0.1% (v/w) BSA and 1 mM $CaCl_2$ were added before use. Mast cells were chemically activated by adding a protein kinase C activator, 50 nM phorbol 12-myristate 13-acetate (PMA), and a calcium ionophore, 500 nM A23187, 0.1% (v/w) BSA, in SG buffer and equilibrated to 37 °C. Prior to activation cells were washed twice with SG buffer (containing BSA and $CaCl_2$). Cells were activated for a period of 2 h. HMC-1 cells were lysed using RIPA buffer (150 mM sodium chloride, 0.5% sodium deoxycholate, 0.1% SDS, 50 mM Tris, 1% Triton X, pH 8.0) containing protease inhibitors. Cells were agitated for 30 min at 4 °C in cell lysis buffer. The solution was centrifuged, and the supernatant was collected and stored at −20 °C until further analysis.

Flow cytometry

Expression of CS by HMC-1 cells was evaluated by flow cytometry. HMC-1 cells, suspended in sterile SG buffer at a concentration of 3×10^6 cells/ml, were analyzed in either their resting or chemically activated state (PMA/A23187). Cells were incubated in each condition for 2 h at 37 °C, and then washed in Dulbecco's PBS (DPBS) and centrifuged at 1200 rpm for 5 min. Cells were then fixed and half of the cells were permeabilized using 300 mM sucrose, 50 mM NaCl, 3 mM $MgCl_2$, 2 mM HEPES, 0.5% (w/v) Triton X-100 for 5 min on ice and blocked using 1% BSA/DPBS for 20 min at room temperature. 500 μl of cell suspension (5×10^5 cells) was incubated with primary antibodies

for 16 h at 4 °C. Primary antibodies included mouse monoclonal anti–chondroitin-4 sulfate stub (clone 2B6, 1:500), mouse monoclonal anti-CS type A and C antibody (clone CS-56, Sigma Aldrich, 1:500), rabbit polyclonal anti-HYAL1 (ab103977, Abcam, 1:100), rabbit polyclonal anti-HYAL4 (ab116547, Abcam, 1:100), and isotype controls, mouse IgM or rabbit Ig (Invitrogen, 1:500). Cells were then incubated with Alexa Fluor 488–conjugated secondary antibodies (1:500, goat anti-mouse IgG/IgM) for 30 min at room temperature and analyzed using a flow cytometer (BD Biosciences) with 1×10^4 events collected per sample. Data were analyzed using the commercial software, FCS 4 Express.

Immuno-EM

HMC-1 cells were fixed for 16 h in 2.5% glutaraldehyde with 4% paraformaldehyde in Sorensen's buffer at 4 °C. Cells were then washed in Sorensen's buffer before being embedded in agar (1% in Sorensen's buffer). Cells were then fixed in 1% osmium tetroxide, followed by dehydration in a series of ethanol washes (ddH_2O, 30% EtOH, 50% EtOH, 70% EtOH, 80%, 90%, 95%, 100% ×3, 20 min). Samples were transferred into embedding resin (LR White resin, ProSciTech Australia) through a series of ethanol:resin solutions (3:1 100% EtOH: resin, 1:1, 1:3, 100% resin ×3, 2 h). Samples embedded in the resin were then allowed to polymerize at 60 °C for 24 h. Specimens were sectioned (Leica EM UC6) and sections were washed in ddH_2O then DPBS before blocking for nonspecific binding (1% (w/v) BSA in Tris-buffered saline (20 mM Tris base, 136 mM NaCl, pH 7.6) with 0.1% (v/v) Tween 20 (TBST)). Sections were probed with antibody clone 2B6 (1:500, 1% BSA/TBST) for 2 h at room temperature. Sections were then probed with 12 nm gold secondary antibody (goat anti-mouse IgG/IgM, 1:50, Abcam). Sections were then washed with DPBS and ddH_2O and allowed to air dry before imaging. Sections were imaged with a transmission electron microscope (JEOL1400, 100 kV).

Immunohistochemistry

Human skin samples were collected by Concord Hospital (New South Wales, Australia) under ethics HREC/14/CRGH/173 and were conducted in strict accordance with the Declaration of Helsinki Principles. Following collection, samples were fixed for 48 h in 4% paraformaldehyde at 4 °C. Following fixation, samples were placed in 70% EtOH and processed as described previously (22, 27). Briefly, paraffin-embedded samples were sectioned (4 μm) and stained for analysis as follows. Sections were washed twice, 5 min each, with xylene to remove paraffin and the slides were immersed in a series of ethanol solutions for 3 min each (twice in 100% (v/v), once in 95% (v/v), once in 70% (v/v)) followed by several exchanges of water. Histological characterization was undertaken using toluidine blue and immunohistological methods. Following rehydration, sections were stained with toluidine blue solution (pH 2.0) for 2 min, washed in reverse osmosis water three times, dipped into 95% EtOH, followed by 100% EtOH twice, cleared in xylene, and mounted. Antigen epitope retrieval was undertaken by immersing the slides, following rehydration, in 0.01 M sodium citrate (pH 6), followed by heat treatment in a decloaking chamber (Applied Medical, Rancho Santa Margarita, CA) at 120 °C for 4 min. The slides were then rinsed with deionized water followed by blocking with 3% (v/v) H_2O_2 for 5 min. Some slides were also treated with C'ase ABC (0.05 units/ml) in 0.1 M Tris acetate buffer (pH 8.0) for 3 h at 37 °C. The slides were washed with TBST and then blocked with 1% (w/v) BSA in TBST for 1 h at room temperature. The slides were incubated with primary antibodies diluted in 1% w/v BSA in TBST at 4 °C for 16 h. Primary antibodies included mouse monoclonal anti–mast cell tryptase (clone AA1, Abcam, 0.1 mg/ml), mouse monoclonal anti–chondroitin-4 sulfate stub (clone 2B6, 1:500), mouse monoclonal anti–chondroitin-6 sulfate stub (clone 3B3, 1:500), and rabbit polyclonal anti-HYAL4 (Abcam, 1:100). Slides were then washed twice with TBST before incubating with the appropriate biotinylated secondary antibodies (GE Healthcare, 1:500) for 1 h at room temperature. The slides were washed twice with TBST then incubated for 30 min with streptavidin-HRP (1:250), rinsed four times with TBST before color development with NovaRED™ chromogen stain (Vector Laboratories, Burlingame CA, USA). The slides were then counterstained with hematoxylin (Gill's No. 3, Vector Laboratories, Burlingame CA) for 6 s and rinsed with deionized water. Slides were dehydrated through graded ethanol series and mounted.

Western blot analysis

HMC-1 cell lysate was electrophoresed in 3–8% (w/v) Tris acetate gels (Invitrogen) under reducing conditions (0.1 M dithiothreitol) using Tris acetate buffer (50 mM tricine, 50 mM Tris, 0.1% (w/v) SDS, pH 8.24) at 160 V for 45 min. A series of molecular mass markers (Precision Plus All Blue, Bio-Rad) was electrophoresed on each gel. Samples were then transferred to PVDF membrane using transfer buffer (5 mM bicine, 5 mM Bis-Tris, 0.2 mM EDTA, 50 μg/ml SDS, 1% (v/v) methanol, pH 7.2) in a semidry blotter at 300 mA and 20 V for 60 min. The membrane was blocked with 1% (w/v) BSA in TBST for 2 h at 25 °C followed by incubation with primary antibody (HYAL4, ab116547, Abcam) diluted in 1% (w/v) BSA in TBST for 16 h at 4 °C. The membrane was subsequently rinsed with TBST, incubated with secondary HRP-conjugated antibodies (1:50,000) for 45 min at 25 °C, and rinsed with TBST and TBS before being imaged using chemiluminescence reagent (Femto reagent kit, Pierce) and X-ray film.

Enzyme-linked immunosorbent assay (ELISA)

For the detection of CS chain or stub epitopes biotinylated CS, CS-A, or CS-D (20 μg/ml) or model CSPGs including ACAN, purified from bovine nasal cartilage (Sigma, 10 μg/ml based on Coomassie Blue protein assay), or recombinant serglycin (SGN), purified by anion exchange chromatography (42), were digested with HYAL1 (1 μg/ml, 50 mM sodium acetate, pH 4), HYAL4 (0.2 μg/μg protein, 50 mM sodium acetate, pH 5), or C'ase ABC (0.05 units/ml, 100 mM Tris acetate, pH 8) for 16 h at 37 °C. For the generation of CS stub epitopes over time samples were prepared to treat 0.5 μg GAG/ml (based on DMMB assay). Samples were digested with either C'ase ABC (0.01 units/mg protein, 100 mM Tris acetate, pH 8) or HYAL4 (0.2 μg/μg protein, 50 mM sodium acetate, pH 5) for various time periods

(0–720 min) at 37 °C. At each time point, samples were incubated at 100 °C for 5 min to inactivate the enzyme and then stored at −20 °C until analysis. Samples were coated onto high-binding 96-well ELISA plates (Greiner, Kremsmünster, Australia) for PG samples or streptavidin-coated 96-well plate (Nunc) for the biotinylated-CS for 2 h at room temperature. Wells were rinsed twice with DPBS followed by blocking with 0.1% (w/v) casein in DPBS for 1 h at 25 °C. Wells were rinsed twice with DPBS with 1% (v/v) Tween 20 (PBST) followed by incubation with primary antibodies diluted in 0.1% (w/v) casein in DPBS for 2 h at room temperature. Primary antibodies include CS-56, 1B5, 2B6, and 3B3, as described above. Wells were rinsed twice with PBST followed by incubation with biotinylated secondary antibodies (anti-mouse Ig or anti-rabbit Ig, 1:1000), followed by streptavidin horseradish peroxidase (1:500). Immunoreactivity was detected using the colorimetric substrate 2,2-azinodi-(3-ethylbenzthiazoline sulfonic acid), and absorbance was measured at 405 nm.

Depolymerization and composition of GAGs by HYAL4

FITC-labeled GAG preparations, including CS-A, CS-C, CS-D, and HA, were prepared as described (48). All the FITC-labeled GAGs were sensitive to at least C'ase ABC and can be degraded into small oligosaccharides as examined by gel filtration on a column of Superdex 200 (data not shown). FITC-labeled CS and HA were analyzed by gel filtration HPLC on a column of Superdex 200 before and after incubation with human HYAL4 (R&D Systems) and monitored by measuring the fluorescent intensity with excitation and emission wavelengths of 490 and 520 nm, respectively. GAGs from within the CS repeating disaccharide region and the linkage region of model CSPGs were also prepared and analyzed following treatment with mouse HYAL4 and C'ase ABC. Model CSPGs included ACAN derived from bovine nasal cartilage (Sigma-Aldrich), salmon nasal cartilage (Ichimaru Pharcos Co., Gifu, Japan), and recombinant SGN. For analysis of oligosaccharides within the CS repeating disaccharide region, PGs were treated with HYAL4 or C'ase ABC followed by labeling with 2-aminobenzamide (2AB). For analysis of oligosaccharides from the linkage region, PGs were alkaline-treated to release the GAGs from the PG protein core and labeled with 2AB (49). The labeled GAGs were then treated with either mouse HYAL4 or C'ase ABC. Labeled CS oligosaccharides from the CS repeating disaccharide region or the linkage region were analyzed by gel filtration HPLC. Composition of the oligosaccharides within the linkage region were further analyzed by anion-exchange HPLC on an amine-bound silica PA-G column (YMC Co., Kyoto, Japan) using a linear gradient of NaH_2PO_4 as described previously (49).

Author contributions—B. L. F., S. M., M. S. L., S. Y., and J. M. W. conceptualization; B. L. F., S. M., M. S. L., R. P. K., S. Y., and J. M. W. resources; B. L. F., S. M., and R. P. K. data curation; B. L. F., S. M., M. S. L., R. L. O., R. P. K., S. Y., and J. M. W. formal analysis; B. L. F., S. M., M. S. L., R. P. K., S. Y., and J. M. W. methodology; B. L. F., S. Y., and J. M. W. writing-original draft; B. L. F. project administration; B. L. F., S. M., M. S. L., R. L. O., R. P. K., S. Y., and J. M. W. writing-review and editing; S. M. investigation.

Acknowledgments—We acknowledge Professor Bruce Caterson (Cardiff University, UK), for the gift of the1B5, 2B6, and 3B3 hybridoma culture supernatants. We thank Professor Peter Maitz and Dr. Zhe Li (Burns Unit, Concord Repatriation General Hospital, Concord, Australia) for collection of the donated skin samples.

References

1. Metcalfe, D. D., Baram, D., and Mekori, Y. A. (1997) Mast cells. *Physiol. Rev.* **77,** 1033–1079 CrossRef Medline
2. Wernersson, S., and Pejler, G. (2014) Mast cell secretory granules: Armed for battle. *Nat. Rev. Immunol.* **14,** 478–494 CrossRef Medline
3. Ringvall, M., Rönnberg, E., Wernersson, S., Duelli, A., Henningsson, F., Åbrink, M., García-Faroldi, G., Fajardo, I., and Pejler, G. (2008) Serotonin and histamine storage in mast cell secretory granules is dependent on serglycin proteoglycan. *J. Allergy Clin. Immunol.* **121,** 1020–1026 CrossRef Medline
4. Forsberg, E., Pejler, G., Ringvall, M., Lunderius, C., Tomasini-Johansson, B., Kusche-Gullberg, M., Eriksson, I., Ledin, J., Hellman, L., and Kjellén, L. (1999) Abnormal mast cells in mice deficient in a heparin-synthesizing enzyme. *Nature* **400,** 773–776 CrossRef Medline
5. Humphries, D. E., Wong, G. W., Friend, D. S., Gurish, M. F., Qiu, W.-T., Huang, C., Sharpe, A. H., and Stevens, R. L. (1999) Heparin is essential for the storage of specific granule proteases in mast cells. *Nature* **400,** 769–772 CrossRef Medline
6. Ohtake-Niimi, S., Kondo, S., Ito, T., Kakehi, S., Ohta, T., Habuchi, H., Kimata, K., and Habuchi, O. (2010) Mice deficient in *N*-acetylgalactosamine 4-sulfate 6-*O*-sulfotransferase are unable to synthesize chondroitin/dermatan sulfate containing *N*-acetylgalactosamine 4,6-bissulfate residues and exhibit decreased protease activity in bone marrow-derived mast cells. *J. Biol. Chem.* **285,** 20793–20805 CrossRef Medline
7. Rönnberg, E., Melo, F. R., and Pejler, G. (2012) Mast cell proteoglycans. *J. Histochem. Cytochem.* **60,** 950–962 CrossRef Medline
8. Kolset, S. O., and Gallagher, J. T. (1990) Proteoglycans in haemopoietic cells. *Biochim. Biophys. Acta* **1032,** 191–211 CrossRef Medline
9. Stevens, R. L., Fox, C. C., Lichtenstein, L. M., and Austen, K. F. (1988) Identification of chondroitin sulfate E proteoglycans and heparin proteoglycans in the secretory granules of human lung mast cells. *Proc. Natl. Acad. Sci. U.S.A.* **85,** 2284–2287 CrossRef Medline
10. Kjellén, L., Pettersson, I., Lillhager, P., Steen, M. L., Pettersson, U., Lehtonen, P., Karlsson, T., Ruoslahti, E., and Hellman, L. (1989) Primary structure of a mouse mastocytoma proteoglycan core protein. *Biochem. J.* **263,** 105–113 CrossRef Medline
11. Stevens, R. L., Lee, T. D., Seldin, D. C., Austen, K. F., Befus, A. D., and Bienenstock, J. (1986) Intestinal mucosal mast cells from rats infected with Nippostrongylus brasiliensis contain protease-resistant chondroitin sulfate di-B proteoglycans. *J. Immunol.* **137,** 291–295 Medline
12. Thompson, H. L., Schulman, E. S., and Metcalfe, D. D. (1988) Identification of chondroitin sulfate E in human lung mast cells. *J. Immunol.* **140,** 2708–2713 Medline
13. Mulloy, B., Lever, R., and Page, C. P. (2017) Mast cell glycosaminoglycans. *Glycoconj. J.* **34,** 351–361 CrossRef Medline
14. Higashi, N., Waki, M., Sue, M., Kogane, Y., Shida, H., Tsunekawa, N., Hasan, A., Sato, T., Kitahara, A., Kasaoka, T., Hayakawa, Y., Nakajima, M., and Irimura, T. (2014) Heparanase-mediated cleavage of macromolecular heparin accelerates release of granular components of mast cells from extracellular matrices. *Biochem. J.* **458,** 291–299 CrossRef Medline
15. Avnur, Z., and Geiger, B. (1984) Immunocytochemical localization of native chondroitin-sulfate in tissues and cultured cells using specific monoclonal antibody. *Cell* **38,** 811–822 CrossRef Medline
16. Ito, Y., Hikino, M., Yajima, Y., Mikami, T., Sirko, S., von Holst, A., Faissner, A., Fukui, S., and Sugahara, K. (2005) Structural characterization of the epitopes of the monoclonal antibodies 473HD, CS-56, and MO-225 specific for chondroitin sulfate D-type using the oligosaccharide library. *Glycobiology* **15,** 593–603 CrossRef Medline

17. Yamagata, M., Kimata, K., Oike, Y., Tani, K., Maeda, N., Yoshida, K., Shimomura, Y., Yoneda, M., and Suzuki, S. (1987) A monoclonal antibody that specifically recognizes a glucuronic acid 2-sulfate-containing determinant in intact chondroitin sulfate chain. *J. Biol. Chem.* **262,** 4146–4152 Medline
18. Watanabe, I., Hikita, T., Mizuno, H., Sekita, R., Minami, A., Ishii, A., Minamisawa, Y., Suzuki, K., Maeda, H., Hidari, K. I. P. J., and Suzuki, T. (2015) Isolation and characterization of monoclonal antibodies specific for chondroitin sulfate E. *Glycobiology* **25,** 953–962 CrossRef Medline
19. Couchman, J. R., Caterson, B., Christner, J. E., and Baker, J. R. (1984) Mapping by monoclonal antibody detection of glycosaminoglycans in connective tissues. *Nature* **307,** 650–652 CrossRef Medline
20. Caterson, B., Christner, J. E., Baker, J. R., and Couchman, J. R. (1985) Production and characterization of monoclonal antibodies directed against connective tissue proteoglycans. *Fed. Proc.* **44,** 386–393 Medline
21. Caterson, B., Mahmoodian, F., Sorrell, J. M., Hardingham, T. E., Bayliss, M. T., Carney, S. L., Ratcliffe, A., and Muir, H. (1990) Modulation of native chondroitin sulphate structure in tissue development and in disease. *J. Cell Sci.* **97,** 411–417 Medline
22. Farrugia, B. L., Whitelock, J. M., O'Grady, R., Caterson, B., and Lord, M. S. (2016) Mast cells produce a unique chondroitin sulfate epitope. *J. Histochem. Cytochem.* **64,** 85–98 CrossRef Medline
23. Prabhakar, V., and Sasisekharan, R. (2006) The biosynthesis and catabolism of galactosaminoglycans. in *Advances in Pharmacology* (Nicola, V., ed), Vol. 53, pp. 69–115, Academic Press, Cambridge, MA CrossRef
24. Kaneiwa, T., Mizumoto, S., Sugahara, K., and Yamada, S. (2010) Identification of human hyaluronidase-4 as a novel chondroitin sulfate hydrolase that preferentially cleaves the galactosaminidic linkage in the trisulfated tetrasaccharide sequence. *Glycobiology* **20,** 300–309 CrossRef Medline
25. Honda, T., Kaneiwa, T., Mizumoto, S., Sugahara, K., and Yamada, S. (2012) Hyaluronidases have strong hydrolytic activity toward chondroitin 4-sulfate comparable to that for hyaluronan. *Biomolecules* **2,** 549–563 CrossRef Medline
26. Csóka, A. B., Scherer, S. W., and Stern, R. (1999) Expression analysis of six paralogous human hyaluronidase genes clustered on chromosomes 3p21 and 7q31. *Genomics* **60,** 356–361 CrossRef Medline
27. Farrugia, B. L., Whitelock, J. M., Jung, M., McGrath, B., O'Grady, R. L., McCarthy, S. J., and Lord, M. S. (2014) The localisation of inflammatory cells and expression of associated proteoglycans in response to implanted chitosan. *Biomaterials* **35,** 1462–1477 CrossRef Medline
28. Hayes, A. J., Tudor, D., Nowell, M. A., Caterson, B., and Hughes, C. E. (2008) Chondroitin sulfate sulfation motifs as putative biomarkers for isolation of articular cartilage progenitor cells. *J. Histochem. Cytochem.* **56,** 125–138 CrossRef Medline
29. Melrose, J., Isaacs, M. D., Smith, S. M., Hughes, C. E., Little, C. B., Caterson, B., and Hayes, A. J. (2012) Chondroitin sulphate and heparan sulphate sulphation motifs and their proteoglycans are involved in articular cartilage formation during human foetal knee joint development. *Histochem. Cell Biol.* **138,** 461–475 CrossRef Medline
30. Sorrell, J. M., Mahmoodian, F., Schafer, I. A., Davis, B., and Caterson, B. (1990) Identification of monoclonal antibodies that recognize novel epitopes in native chondroitin/dermatan sulfate glycosaminoglycan chains: Their use in mapping functionally distinct domains of human skin. *J. Histochem. Cytochem.* **38,** 393–402 CrossRef Medline
31. Slater, R. R., Jr., Bayliss, M. T., Lachiewicz, P. F., Visco, D. M., and Caterson, B. (1995) Monoclonal antibodies that detect biochemical markers of arthritis in humans. *Arthritis Rheum.* **38,** 655–659 CrossRef Medline
32. Asari, A., Akizuki, S., Itoh, T., Kominami, E., and Uchiyama, Y. (1996) Human osteoarthritic cartilage exhibits the 2B6 epitope without pretreatment with chondroitinase ABC. *Osteoarthritis Cartilage* **4,** 149–152 CrossRef Medline
33. Gotis-Graham, I., and McNeil, H. P. (1997) Mast cell responses in rheumatoid synovium. Association of the MCTC subset with matrix turnover and clinical progression. *Arthritis Rheum.* **40,** 479–489 CrossRef Medline
34. Dean, G., Hoyland, J. A., Denton, J., Donn, R. P., and Freemont, A. J. (1993) Mast cells in the synovium and synovial fluid in osteoarthritis. *Rheumatology* **32,** 671–675 CrossRef Medline
35. Martin, D. C., Atmuri, V., Hemming, R. J., Farley, J., Mort, J. S., Byers, S., Hombach-Klonisch, S., Csoka, A. B., Stern, R., and Triggs-Raine, B. L. (2008) A mouse model of human mucopolysaccharidosis IX exhibits osteoarthritis. *Hum. Mol. Gen.* **17,** 1904–1915 CrossRef Medline
36. Bourguignon, V., and Flamion, B. (2016) Respective roles of hyaluronidases 1 and 2 in endogenous hyaluronan turnover. *FASEB J.* **30,** 2108–2114 CrossRef Medline
37. Gushulak, L., Hemming, R., Martin, D., Seyrantepe, V., Pshezhetsky, A., and Triggs-Raine, B. (2012) Hyaluronidase 1 and β-hexosaminidase have redundant functions in hyaluronan and chondroitin sulfate degradation. *J. Biol. Chem.* **287,** 16689–16697 CrossRef Medline
38. Petrey, A., and de la Motte, C. (2014) Hyaluronan, a crucial regulator of inflammation. *Front. Immunol.* **5,** 101 CrossRef Medline
39. Nagaya, H., Ymagata, T., Ymagata, S., Iyoda, K., Ito, H., Hasegawa, Y., and Iwata, H. (1999) Examination of synovial fluid and serum hyaluronidase activity as a joint marker in rheumatoid arthritis and osteoarthritis patients (by zymography). *Ann. Rheum. Dis.* **58,** 186–188 CrossRef Medline
40. Muto, J., Morioka, Y., Yamasaki, K., Kim, M., Garcia, A., Carlin, A. F., Varki, A., and Gallo, R. L. (2014) Hyaluronan digestion controls DC migration from the skin. *J. Clin. Invest.* **124,** 1309–1319 CrossRef Medline
41. Theoharides, T. C., Alysandratos, K.-D., Angelidou, A., Delivanis, D.-A., Sismanopoulos, N., Zhang, B., Asadi, S., Vasiadi, M., Weng, Z., Miniati, A., and Kalogeromitros, D. (2012) Mast cells and inflammation. *Biochim. Biophys. Acta* **1822,** 21–33 CrossRef Medline
42. Lord, M. S., Cheng, B., Tang, F., Lyons, J. G., Rnjak-Kovacina, J., and Whitelock, J. M. (2016) Bioengineered human heparin with anticoagulant activity. *Metab. Eng.* **38,** 105–114 CrossRef Medline
43. Åbrink, M, Grujic, M., and Pejler, G. (2004) Serglycin is essential for maturation of mast cell secretory granule. *J. Biol. Chem.* **279,** 40897–40905 CrossRef Medline
44. Hallgren, J., Spillmann, D., and Pejler, G. (2001) Structural requirements and mechanism for heparin-induced activation of a recombinant mouse mast cell tryptase, mouse mast cell protease-6. *J. Biol. Chem.* **276,** 42774–42781 CrossRef Medline
45. Bashkin, P., Razin, E., Eldor, A., and Vlodavsky, I. (1990) Degranulating mast cells secrete an endoglycosidase that degrades heparan sulfate in subendothelial extracellular matrix. *Blood* **75,** 2204–2212 Medline
46. Wang, B., Jia, J., Zhang, X., Zcharia, E., Vlodavsky, I., Pejler, G., and Li, J.-P. (2011) Heparanase affects secretory granule homeostasis of murine mast cells through degrading heparin. *J. Allergy Clin. Immunol.* **128,** 1310–1317.e1318 CrossRef Medline
47. Kaneiwa, T., Miyazaki, A., Kogawa, R., Mizumoto, S., Sugahara, K., and Yamada, S. (2012) Identification of amino acid residues required for the substrate specificity of human and mouse chondroitin sulfate hydrolase (conventional hyaluronidase-4). *J. Biol. Chem.* **287,** 42119–42128 CrossRef Medline
48. Kaneiwa, T., Yamada, S., Mizumoto, S., Montaño, A. M., Mitani, S., and Sugahara, K. (2008) Identification of a novel chondroitin hydrolase in *Caenorhabditis elegans*. *J. Biol. Chem.* **283,** 14971–14979 CrossRef Medline
49. Mizumoto, S., and Sugahara, K. (2012) Glycosaminoglycan chain analysis and characterization (glycosylation/epimerization). in *Proteoglycans: Methods and Protocols* (Rédini, F., ed), pp. 99–115, Humana Press, Totowa, NJ CrossRef